JOURNAL OF GEOPHYSICAL RESEARCH, VOL. 85, NO. C3, PAGES 1548-1552, MARCH 20, 1980

# Narrow-Band Nonlinear Sea Waves

M. AZIZ TAYFUN

*College of Engineering and Petroleum, Kuwait University, Kuwait*

Probabilistic description of nonlinear waves with a narrow-band spectrum is simplified to a form in which each realization of the surface displacement becomes an amplitude-modulated Stokes wave with a mean frequency and random phase. Under appropriate conditions this simplification provides a convenient yet rigorous means of describing nonlinear effects on sea surface properties in a semiclosed or closed form. In particular, it is shown that surface displacements are non-Gaussian and skewed, as was previously predicted by the Gram-Charlier approximation; that wave heights are Rayleigh distributed, just as in the linear case; and that crests are non-Rayleigh.

## INTRODUCTION

Although a great deal of recent progress has been made on the theory of nonlinear sea waves, the complicated form of higher-order corrections to linear first-order representation of a random sea surface impedes further development of the nonlinear theory in certain aspects. In particular, statistical properties and distributions relevant to a wave field, such as surface displacements, wave crests, and heights, do not appear to be amenable to a theoretical treatment in contrast with the linear theory, which asserts that the free surface is Gaussian, and wave heights and crests are Rayleigh distributed provided that the underlying spectrum is narrow band. The nonlinearity of the wave profile introduces a skewness to the Gaussian description of the free surface, a feature predicted by the Gram-Charlier series solution of *Longuet-Higgins* [1963]. On the other hand, the solution in terms of the Gram-Charlier series is an approximation which remains to be fully tested, and it does not appear likely that the theoretical understanding can be extended to other wave field properties, such as wave heights, crests, etc. At present, empirical or numerical simulation of some of these properties as demonstrated by R. T. Hudspeth (unpublished data, 1975) and *Hudspeth and Chen* [1979] constitutes a practical alternative to the analytical approach.

This paper is an attempt to simplify the probabilistic modeling of nonlinear random waves to a form which would be more amenable to numerical or theoretical treatments under appropriate conditions. Specifically, when the first-order structure of sea surface is narrow-band Gaussian, the stochastic representation of the surface can be reduced to a familiar form in which each realization is an amplitude-modulated Stokian wave profile with a mean frequency and random phase. Derivation of probability densities of surface displacements, wave heights, and crests immediately follows from the physical picture provided by this simplification and by using standard statistical techniques.

## NARROW-BAND APPROXIMATION

The surface displacement satisfying the usual equations of free wave motion to second order in a unidirectional sea can be represented by [e.g., *Longuet-Higgins*, 1963]

$$\eta(x,t) = \sum_{n=1}^{N} c_n \cos(\chi_n + \epsilon_n) - \frac{2}{g} \sum_{m,n \geq m}^{N} c_n c_m \omega_n (\omega_n - \omega_m) \cos(\chi_n - \chi_m + \epsilon_n - \epsilon_m) - \frac{1}{2g} \sum_{n,m}^{N} c_n c_m \omega_n \omega_m \cos(\chi_n - \chi_m + \epsilon_n - \epsilon_m) + \frac{1}{g} \sum_{n,m}^{N} c_n c_m \omega_m^2 \cos(\chi_n + \epsilon_n) \cos(\chi_m + \epsilon_m) \tag{1}$$

where

$$\omega_n^2 = gk_n \qquad \chi_n = k_n x - \omega_n t \tag{2}$$

and the $\epsilon_n$ denote random phases uniformly distributed over an interval of $2\pi$.

The first-order spectrum is given by the leading term of (1), that is,

$$\frac{1}{2} \sum_{\omega_n \ni \delta\omega} c_n^2 \simeq S(\omega)\, d\omega \qquad \delta\omega = (\omega, \omega + d\omega) \tag{3}$$

The second-order corrections to (3) due to the remaining terms of (1) are negligible, being proportional to $g^{-2}$. The $j$th spectral moment is defined as

$$\mu_j = \int_0^\infty \omega^j S(\omega)\, d\omega \simeq \frac{1}{2} \sum_{n=1}^{N} \omega_n^j c_n^2 \tag{4}$$

In particular, $\mu_0$ and $\mu_1/\mu_0 = \omega_0$ represent the first-order variance and mean frequency, respectively. The spectrum is considered to be narrow band if [*Longuet-Higgins*, 1975]

$$\nu^2 = (\mu_2/\mu_0\, \omega_0^2) - 1 \ll 1 \tag{5}$$

Under this condition we can write

$$\eta_1 = \sum_n c_n \cos(\chi_n + \epsilon_n) = a(x,t) \cos(\chi_0 + \phi) \tag{6}$$

where $a(x, t)$ and $\phi(x, t)$ represent the amplitude and phase functions, respectively, defined by

$$a \exp(i\phi) = \sum_n c_n \exp[i(\chi_n - \chi_0 + \epsilon_n)] \tag{7}$$

The first-order process $\eta_1$ is asymptotically Gaussian as the number of terms, $N$, of cosine functions approaches infinity. Under this limiting condition it may be more appropriate to express (6) as a random Fourier-Stieltjes integral. However, in the actual application of (6) to gravity waves and other related phenomena the Gaussian approximation is satisfied remarkably well for a finite sum of cosine terms [*Lyon*, 1970; *Yang*, 1973]. In fact, if we do not concern ourselves with extremal statistics which depend highly on the tail ends of a distribution, $N$ could be as small as 20. Consequently, given that the



Paper number 9C1606.
0148-0227/80/009C-1606$01.00

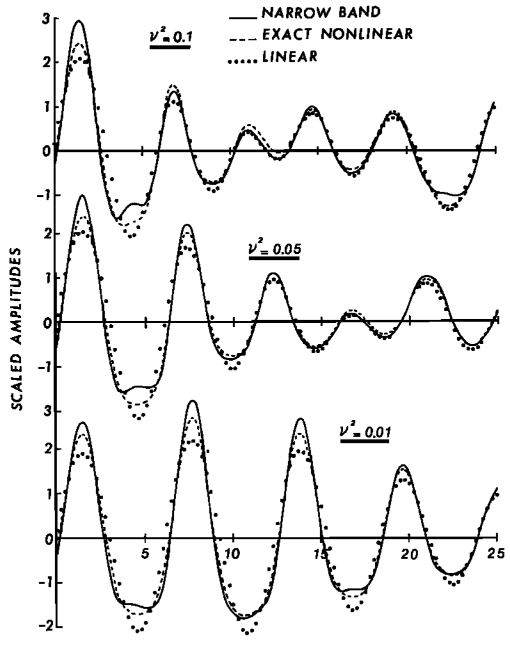


Fig. 1. Comparison of linear and nonlinear realizations with narrow-band approximation for $k_0\mu_0{}^{1/2} = 0.2$.

probability structure of (6) is approximated by the Gaussian law, the amplitude process $a(x, t)$ is Rayleigh distributed [*Rice*, 1954; *Middleton*, 1960], that is,

$$f_a(u) = (u/\mu_0)\exp(-u^2/2\mu_0) \qquad u \ge 0 \qquad (8)$$

The expected number of crests per unit time is given by $(2\pi)^{-1}(\mu_4/\mu_2)^{1/2}$ [*Rice*, 1954]. Since the expected number of crests over the mean period $2\pi/\omega_0$ is $(\mu_4/\mu_2\omega_0{}^2)^{1/2} \simeq 1$, it follows from (5) that

$$\mu_2 - \mu_0\omega_0{}^2 = \mu_0\omega_0{}^2\nu^2 \qquad \mu_4 - \mu_0\omega_0{}^4 \simeq \mu_0\omega_0{}^4\nu^2 \qquad (9)$$

Consider now the second term of (1). Its magnitude can be shown to be less than

$$\frac{2}{g}\left\{\sum_{n,m}^{N} c_n c_m(\omega_n+\omega_0)|\omega_n-\omega_0| + \sum_{n,m}^{N} c_n c_m(\omega_n-\omega_0)|\omega_m-\omega_0| + \sum_{n,m}^{N} c_n c_m(\omega_n-\omega_0)|\omega_m-\omega_0|\right\} \le 4Nk_0\mu_0\nu(1+\nu) \qquad (10)$$

where $k_0 = \omega_0{}^2/g$, and the right-hand side of the expression follows from the Schwarz inequality and (9). Therefore the contribution of the second term of (1) to $\eta$ is at most $o(k_0\mu_0\nu)$. Next, by expanding the cosine term and letting $\omega_n = \omega_n + \omega_0 - \omega_0$ and $\omega_m = \omega_m + \omega_0 - \omega_0$ the third term of (1) can be written in the equivalent form

$$-\frac{1}{2g}\left\{\omega_0{}^2a^2(x,t) + \left[\sum_n c_n(\omega_n-\omega_0)\cos(\chi_n+\epsilon_n)\right]^2 + \left[\sum_n c_n(\omega_n-\omega_0)\sin(\chi_n+\epsilon_n)\right]^2\right\} \qquad (11)$$

With the contribution of the last two terms of (11) being bounded by $2Nk_0\mu_0\nu^2$ by the Schwarz inequality, the third term of (1) reduces to

$$-\tfrac{1}{2}k_0a^2(x,t) + o(k_0\mu_0\nu^2) \qquad (12)$$

Similarly, by setting $\omega_m{}^2 = \omega_m{}^2 + \omega_0{}^2 - \omega_0{}^2$ the last term of (1) can be shown to be

$$k_0a^2(x,t)\cos^2(\chi_0+\phi) + o(k_0\mu_0\nu) \qquad (13)$$

Finally, the substitution of the preceding approximations into (1) provides a narrow-band representation for $\eta$ in the form

$$\eta(x,t) = a(x,t)\cos(\chi_0+\phi) + \tfrac{1}{2}k_0a^2(x,t)\cos 2(\chi_0+\phi) + o(k_0\mu_0\nu) \qquad (14)$$

Each realization of (14) is as an amplitude-modulated Stokian wave with a mean frequency $\omega_0$, wave number $k_0 = \omega_0{}^2/g$, and phase $\phi$. This interpretation offers certain advantages over the exact solution (1). One of these stems from the obvious similarity of (14) to a deterministic Stokes wave. Hence the physical effect of nonlinear corrections disguised in the complicated form of (1) is concisely represented by the second term of (14), which introduces a vertical asymmetry to the linear profile by causing crests to become narrower and sharper and troughs to become longer and shallower. Another advantage is the simple functional form, which is more amenable to numerical and theoretical analyses. In particular, probabilistic description of surface properties, such as displacements, wave crests, and heights, can be derived in a closed or semiclosed form by using standard techniques which evidently fail in view of the intricate form of the exact solution (1).

## VALIDITY OF NARROW-BAND APPROXIMATION

Before we attempt to examine the probabilistic description of various surface properties based on the narrow-band approximation, it is prudent to assess the validity of such an approximation. One possible means of achieving this objective is to simulate and compare explicit realizations of the exact and approximate solutions. Therefore in the following we may proceed to generate samples of the scaled process $\eta/\mu_0{}^{1/2}$ in the time domain by using both (1) and (14). First, note that (14) can be rewritten in the quadratic form

$$z = \eta/\mu_0{}^{1/2} = z_1 + \tfrac{1}{2}k_0\mu_0{}^{1/2}(z_1{}^2 - \bar{z}_1{}^2) + o(k_0\mu_0{}^{1/2}\nu) \qquad (15)$$

where

$$z_1 = \mu_0{}^{-1/2}\sum_{n=1}^{N} c_n\cos(\chi_n+\epsilon_n) \qquad (16)$$

$$\bar{z}_1 = \mu_0{}^{-1/2}\sum_{n=1}^{N} c_n\sin(\chi_n+\epsilon_n) \qquad (17)$$

The simulation for the realizations of (1) and (15) proceeds by choosing a set of $N$ random phases $\epsilon_n$ equally likely over the interval $(0, 2\pi)$ and by defining

$$c_n = \{2S(\omega_n)\Delta\omega_n\}^{1/2} \qquad n = 1, \cdots, N \qquad (18)$$

which represents a discretization of the continuous frequency range into $N$ distinct bands of width $\Delta\omega_n$ and central frequency $\omega_n$. As an example, consider the spectral form

$$\begin{aligned} S(\omega) &= (S_0/\Delta\omega)(\omega + \Delta\omega - 1) \qquad 1 - \Delta\omega \le \omega \le 1 \\ S(\omega) &= -(S_0/\Delta\omega)(\omega - \Delta\omega - 1) \qquad 1 \le \omega \le 1 + \Delta\omega \end{aligned} \qquad (19)$$

with $\mu_0 = \mu_1 = S_0\Delta\omega$, $\mu_2 = S_0\Delta\omega(1 + \Delta\omega^2/6)$, $k_0\mu_0{}^{1/2} = (S_0\Delta\omega)^{1/2}/g$, and $\nu^2 = \Delta\omega^2/6$. The triangular form of (19) with height $S_0$, base width $2\Delta\omega$, and mean frequency $\omega_0 = 1$ rad/s does not necessarily represent a general oceanic situation.

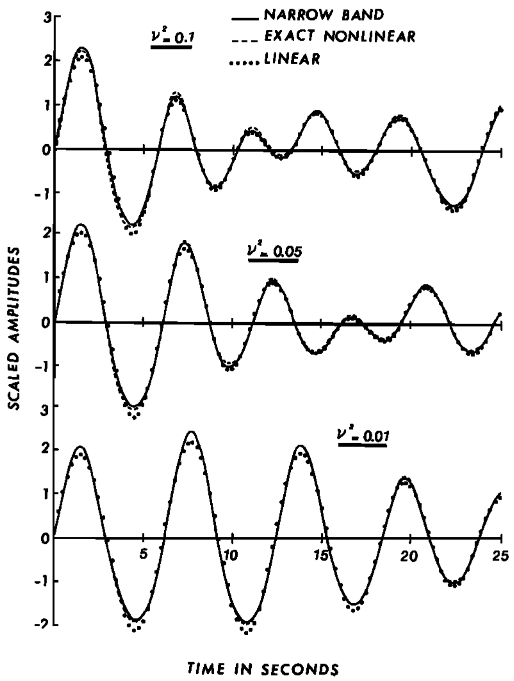


Fig. 2. Comparison of linear and nonlinear realizations with narrow-band approximation for $k_0\mu_0^{1/2} = 0.1$.

Rather, its functional form is convenient in allowing $\nu^2$ and $k_0\mu_0^{1/2}$ to vary in a simple manner. More familiar forms, such as Joint North Sea Wave Project and Pierson-Moskowitz spectra, are either too complex or have an invariant bandwidth $\nu^2$.

Two sets of simulations, corresponding to $k_0\mu_0^{1/2} = 0.1$ and 0.2, were carried out with $N = 20$ and by varying $\Delta\omega$ and thereby $\nu^2$ from 0.1 to 0.01 for each set. Some of the characteristic results are shown in Figures 1 and 2 together with the corresponding linear counterparts computed from (16). The comparison between the nonlinear simulations is very favorable, particularly for small values of both $\nu^2$ and $k_0\mu_0^{1/2}$, for example, $k_0\mu_0^{1/2} = 0.1$ and $\nu^2 = 0.01$. Obviously, this is consistent with the requirement $k_0\mu_0^{1/2}\nu \ll 1$ embedded in the narrow-band approximation (15). For the same reason the comparison becomes increasingly unfavorable for larger values of $k_0\mu_0^{1/2}\nu$, for example, $k_0\mu_0^{1/2} = 0.2$ and $\nu^2 = 0.1$. Consequently, we can conclude that a narrow-band approximation to (1) in the form of (14) or (15) indeed has validity provided that $k_0\mu_0^{1/2}\nu \ll 1$.

In analogy with $ka$ in the deterministic Stokes theory the parameter $k_0\mu_0^{1/2}$ here can be regarded as a measure of steepness for the free surface, particularly as $\nu^2 \to 0$. Obviously, this analogy becomes irrelevant as $\nu^2$ becomes large, because the free surface can no longer be described as an amplitude-modulated wave form. For example, in a wind-generated wave field, where the spectral characteristics of the saturated free surface characterized with sporadic breaking and whitecapping is given by the Phillips spectrum $S(\omega) \simeq \omega^{-5}$ m² s⁻¹ at frequencies above, for example, $\omega = \omega^*$, it can be shown that $\nu > 0.35$, $k_0\mu_0^{1/2} \simeq 0.9$, and $k_0\mu_0^{1/2}\nu > 0.3$ invariably. Therefore the applicability of the narrow-band approximation within a generation area is questionable. However, as waves propagate out of the generation area, or in a decaying wave field, the spectral amplitudes are known to fall below the saturation range values in an increasing manner toward the high-frequency tail. Under these conditions, $\nu^2$ and $k_0\mu_0^{1/2}$ are expected to become progressively small, suggesting that the narrow-band representation would be more appropriate for waves distant from a generation area.

## DISTRIBUTION OF SURFACE DISPLACEMENTS

The second-order surface displacement (15) can be rewritten as

$$\zeta = \eta/\eta_{\rm rms} = \gamma^{-1}\{z_1 + \tfrac{1}{2}k_0\mu_0^{1/2}(z_1^2 - \bar{z}_1^{2})\} \tag{20}$$

where

$$\eta_{\rm rms} = \gamma\mu_0^{1/2} = (1 + k_0^2\mu_0)^{1/2}\mu_0^{1/2} \tag{21}$$

It can be verified that $z_1$ and $\bar{z}_1$ are zero-mean Gaussian with the joint density

$$f_{z_1\bar{z}_1}(u_1, u_2) = (2\pi)^{-1}\exp\{-\tfrac{1}{2}(u_1^2 + u_2^2)\} \quad |u_1|, |u_2| < \infty \tag{22}$$

The cumulative distribution of $\zeta$ is defined as

$$F_\zeta(u) = \text{Prob}\ \{\zeta \le u\}$$
$$= \text{Prob}\ \{z_1 + \tfrac{1}{2}k_0\mu_0^{1/2}(z_1^2 - \bar{z}_1^2) \le \gamma u\} \tag{23}$$

Using (22) and paying appropriate attention to the region of integration implied in (23), we obtain

$$F_\zeta(u) = (2\pi)^{-1}\int_{\alpha(u)}^{\infty} e^{-\tau^2/2}\,\{\text{erf}\,[A(\tau, u) + \beta] + \text{erf}\,[A(\tau, u) - \beta]\}\,d\tau \tag{24}$$

where

$$\beta = 1/2^{1/2}k_0\mu_0^{1/2} \tag{25}$$

$$\alpha(u) = 0 \qquad u \ge -\beta/2^{1/2}\gamma \tag{26}$$

$$\alpha(u) = 2^{1/2}\beta\,\{-(1 + 2^{1/2}\gamma u\beta^{-1})\}^{1/2}$$

otherwise, and

$$A(\tau, u) = \beta(1 + 2^{1/2}\gamma u\beta^{-1} + \tau^2\beta^{-2})^{1/2} \tag{27}$$

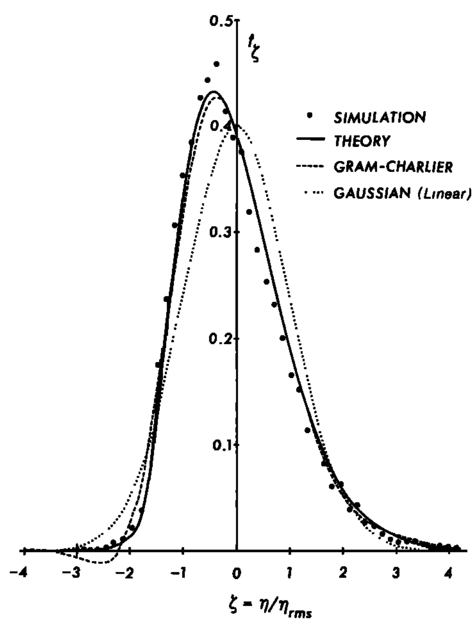


Fig. 3. Probability density of surface displacement for $k_0\mu_0^{1/2} = 0.3$.

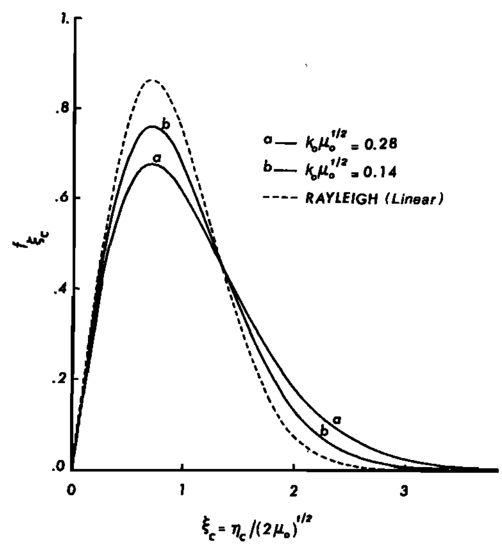


Fig. 4. Probability density of linear and nonlinear crest heights.

The explicit evaluation of $F_\zeta$ or its derivative, which is the probability density $f_\zeta$ of interest here, requires numerical integration. Hence as an illustrative case we let $k_0\mu_0^{1/2} = 0.3$ with the inherent assumption that $k_0\mu_0^{1/2}\,\nu \ll 1$ by virtue of $\nu \ll 1$. The construction of $f_\zeta$ proceeds by computing first $F_\zeta$ with the well-known trapezoidal scheme followed by forward finite differentiation over the interval from $\tau = -4$ to $\tau = 6$, using base points equally spaced by step size $\Delta\tau = 10^{-3}$. The resulting theoretical density $f_\zeta$ is displayed in Figure 3. Also shown for comparison in the same figure is the corresponding empirical density based on $10^4$ realizations of $\zeta$ computed through (20).

An approximation to $f_\zeta$ in terms of the Gram-Charlier series is [*Longuet-Higgins*, 1963]

$$f_\zeta(u) = (2\pi)^{-1/2}e^{-u^2/2}\,(1 + \tfrac{1}{6}\lambda_3 H_3 + \tfrac{1}{24}\lambda_4 H_4 + \tfrac{1}{72}\lambda_3^2 H_6) \qquad (28)$$

where

$$H_3 = u^3 - 3u$$
$$H_4 = u^4 - 6u^2 + 3 \qquad (29)$$
$$H_6 = u^6 - 15u^4 + 45u^2 - 15$$

and the coefficients of skewness and kurtosis corresponding to (20) are

$$\lambda_3 = 3\gamma^{-3}k_0\,\mu_0^{1/2} \qquad (30)$$

$$\lambda_4 = 3\gamma^{-4}\,(1 + 6k_0^2\,\mu_0 + 3k_0^4\,\mu_0^2) - 3 \qquad (31)$$

respectively. The above approximation is also shown in Figure 3 for the case $k_0\mu_0^{1/2} = 0.3$ together with the theoretical result and the Gaussian density corresponding to the linear process $z_1 = \eta_1/\mu_0^{1/2}$ for comparison. First of all, it is evident that the probability structure of the nonlinear process $\zeta$ represented by either the theoretical density or the Gram-Charlier approximation is significantly different from the Gaussian description. This difference is in the form of a skewness imposed on the symmetrical Gaussian form resulting in less likely large negative values and more likely higher positive values of the surface displacement, which is entirely consistent with the vertical asymmetry of the nonlinear profile with sharper narrower crests and longer shallower troughs than those of the linear profile. Recent studies on the probability distribution of the surface displacements, for example, by *Huang and Long* [1979], confirm the validity of this basic skew structure based on extensive empirical field and laboratory data. *Huang and Long* [1979] also examine in detail the accuracy of Gram-Charlier type expansions, with the conclusion that the particular type (28) proposed by *Longuet-Higgins* [1963] works well. This conclusion is also supported here based on the comparison between the Gram-Charlier approximation and the exact solution. It is observed, however, that there are a few points of concern. The first is the negative range of the Gram-Charlier approximation at large negative values of the surface displacement, which is not meaningful and, as was noted by *Huang and Long* [1979], introduces a negative bias. Therefore in applications this bias must be corrected by shifting, normalizing, and centering the expansion to zero mean. Clearly, these operations require a considerable amount of numerical effort, implying that the proper application of the Gram-Charlier approximation is not as straightforward as its simple functional form might suggest. A second point of concern arises also in practice from the possibility that the estimates of $\lambda_3$ and $\lambda_4$ based on field or laboratory data can be unreliable because of sampling fluctuations. This point of concern is not materialized here simply because the coefficients $\lambda_3$ and $\lambda_4$ included in the expansion (28) are exact.

## DISTRIBUTION OF CREST HEIGHTS

Crest heights or, equivalently, maxima associated with the nonlinear wave process (14) are given in a dimensionless form by

$$\xi_c = \hat{a} + (1/2^{1/2})\,k_0\,\mu_0^{1/2}\hat{a}^2 \qquad (32)$$

where $\hat{a} = a/a_{\rm rms}$ with $a_{\rm rms} = (2\mu_0)^{1/2}$ corresponds to the scaled crest height in the linear case. The probability distribution of $\hat{a}$ is the well-known Rayleigh law, that is,

$$f_{\hat{a}}(u) = 2u\exp(-u^2) \qquad u \geq 0 \qquad (33)$$

The density of $\xi_c$ in this case follows easily from (32), (33), and the relation

$$f_{\xi_c}(w) = (du/d\xi_c)f_{\hat{a}}(u)|_{u=\xi_c^{-1}(w)} \qquad (34)$$

as

$$f_{\xi_c}(w) = 2\beta\{1 - (1 + 2w\beta^{-1})^{-1/2}\}$$
$$\cdot\exp\{-\beta^2[-1 + (1 + 2w\beta^{-1})^{1/2}]^2\} \qquad w \geq 0 \qquad (35)$$

with $\beta$ defined by (25).

The probability density represented by (35) is shown in Figure 4 for $k_0\mu_0^{1/2} = 0.28$ and 0.14 together with the conventional Rayleigh form for comparison. It is evident that the densities associated with the nonlinear waves differ from the Rayleigh form in an increasing manner as $k_0\mu_0^{1/2}$ becomes large. The general character of this difference is in the form of a spreading of the density mass toward the higher crests, which is again consistent with the vertical asymmetry of the nonlinear waves with sharper and larger crests than the linear counterparts, that is, $\xi_c - \hat{a} = (1/2^{1/2})k_0\mu_0^{1/2}\,\hat{a}^2 \geq 0$. The area under a density curve to the right of a specified abscissa represents the probability with which the specified level will be exceeded. This probability, simply known as the exceedance probability, is of primary concern in the design of ocean structures such as offshore platforms, breakwaters, and sea walls. What is suggested by the results here is that the Rayleigh density underestimates exceedance probabilities associated with higher crests of engineering design concern.

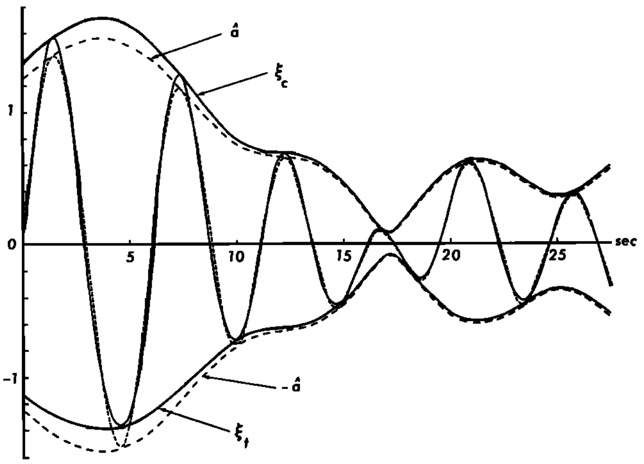


Fig. 5. Envelopes of linear and nonlinear surface displacements for $k_0\mu_0^{1/2} = 0.1$ and $\nu^2 = 0.01$.

## DISTRIBUTION OF WAVE HEIGHTS

The maximum $\xi_c$ defined by (32) is a temporally and spatially homogeneous random process. As such it represents an envelope for each realization of the scaled nonlinear process $\eta/(2\mu_0)^{1/2}$ above still water level. Similarly, each temporal or spatial realization of

$$\xi_t = -\hat{a} + (1/2^{1/2})\, k_0\mu_0^{1/2}\hat{a}^2 \quad (36)$$

is an envelope of surface displacements below still water level. It is well known in the linear case $\eta_1/(2\mu_0)^{1/2}$ that the corresponding envelopes are $\hat{a}$ and $-\hat{a}$, respectively. The linear and nonlinear envelopes defined in the preceding manner can be simulated explicitly, using (32), (36), and

$$\hat{a} = (1/2^{1/2})(z_1^2 + \dot{z}_1^2)^{1/2} \quad (37)$$

This is illustrated in the time domain for the case $k_0\mu_0^{1/2} = 0.1$ and $\nu^2 = 0.01$ in Figure 5, together with the corresponding realizations of the scaled processes $\eta/(2\mu_0)^{1/2}$ and $\eta_1/(2\mu_0)^{1/2}$.

The local wave height at a fixed $x$ or $t$ is defined as the difference between the upper and lower envelopes. Hence in the linear case it is given in a scaled form by

$$\xi = H/H_{rms} = \hat{a} \quad (38)$$

where $H = 2a$ and $H_{rms} = 2(2\mu_0)^{1/2}$. In contrast with the linear case the envelopes $\xi_c$ and $\xi_t$ are not symmetric with respect to still water level. However, both are displaced upward by an equal amount $(1/2^{1/2})k_0\mu_0^{1/2}\hat{a}^2$ so that their difference is exactly the same as that in the linear counterpart. Therefore the scaled nonlinear wave height remains identical with $\xi$ and is distributed according to the Rayleigh probability law (33).

Numerous field observations confirm the validity of the theoretical Rayleigh law, particularly for low and medium wave height ranges. However, a discrepancy between empirical data and the theory is often noted toward the high wave tail, the theory overpredicting the observations. *Forristall* [1978] attributes this discrepancy to the nonlinear, non-Gaussian, and skewed nature of the free surface. On the basis of the preceding results it is evident that these characteristics do not directly result in reducing wave heights in a manner consistent with field observations. A more plausible mechanism is wave breaking, which is a nonlinear effect not directly accounted for in the analytical wave models currently available.

## CONCLUDING REMARKS

Waves distant from a generation area can be approximated in terms of an amplitude-modulated Stokian wave process provided that the underlying first-order spectrum is narrow band. In contrast with the intricate complexity of exact nonlinear solutions, such an approximation constitutes a simpler formulation to study numerically or analytically the nonlinear effects on the statistical description of wave field properties. This was demonstrated here with a number of results on the probability distribution of various surface properties. In particular, it was shown that surface displacements can be described exactly to be non-Gaussian and skewed, wave heights are distributed according to the Rayleigh probability law, and crests are non-Rayleigh, unlike their linear counterparts.

The proposed approximation can easily be extended to other kinematic and dynamic properties of a wave field. Consequently, it should prove to be a useful concept in the statistical modeling of nonlinear waves both in theory and in applications under appropriate conditions.

*Acknowledgments.* The author is indebted to N. E. Huang and C. C. Tung for stimulating his interest in this problem. The study was partially supported by funds from NASA (contract NAS6-3018) and from the Department of Marine Science and Engineering, North Carolina State University.

## REFERENCES


Forristall, G., On the statistical distribution of wave heights in a storm, *J. Geophys. Res., 83*(C5), 2353–2358, 1978.

Huang, N. E., and S. R. Long, A study of the surface elevation probability distribution and statistics of wind generated waves, submitted to *J. Fluid Mech.*, 1979.

Hudspeth, R. T., and M.-C. Chen, Digital simulation of non-linear random waves, *J. Waterway Port Coastal Ocean Div. Amer. Soc. Civil Eng., 105*(*WW1*), 67–85, 1979.

Longuet-Higgins, M. S., The effect of non-linearities on statistical distributions in the theory of sea waves, *J. Fluid Mech., 17*(3), 450–480, 1963.

Longuet-Higgins, M. S., On the joint distribution of the periods and amplitudes of sea waves, *J. Geophys. Res., 80*(18), 2688–2694, 1975.

Lyon, R. H., Statistics of combined sine waves, *J. Acoust. Soc. Amer., 48*, 145–149, 1970.

Middleton, D., *An Introduction to Statistical Communication Theory*, chap. 9, McGraw-Hill, New York, 1960.

Rice, S. O., Mathematical analysis of random noise, in *Selected Papers on Noise and Stochastic Processes*, edited by N. Wax, p. 133, Dover, New York, 1954.

Yang, J.-N., On the normality of simulated random process, *J. Sound Vib., 26*(3), 417–428, 1973.


(Received May 25, 1979;
revised October 1, 1979;
accepted November 6, 1979.)